JOURNAL OF Applied Polymer SCIENCE

Evolution of the Amorphous Fraction of PEEK During Annealing at Atmospheric and High Pressure Above the Glass Transition Temperature

Marion Dasriaux, Sylvie Castagnet, Ludovic Thilly, Laurence Chocinski-Arnault, Séverine A. E. Boyer
Institut P PRIME (UPR 3346 CNRS – ISAE ENSMA – Université de Poitiers,) Chasseneuil-Futuroscope, France
Correspondence to: M. Dasriaux (E-mail: marion.dasriaux@ensma.fr).

ABSTRACT: The constrained fraction of the amorphous phase of semi-crystalline polymers is in an out-of-equilibrium state so that physical aging-like features can be observed (e.g., by calorimetry) even above the glass transition temperature. This was already addressed in the literature in several semi-crystalline polymers at atmospheric pressure. Despite the well-known influence of pressure on molecular mobility, the pressure-sensitivity of these microstructure rearrangements has never been tackled. This study focuses on annealing in highly pressurized Poly-Ether-Ether-Ketone (PEEK), compared with atmospheric pressure. The phenomenon is tracked by *ex-situ* Differential Scanning Calorimetry (DSC). A significant influence of pressure is evidenced, without any complete equivalence with temperature. Indeed, pressure seems to confine rearrangements within spatially limited domains. The stability and coexistence of reorganization processes upon successive annealings is also investigated. Finally, relationships between constrained and free amorphous phase rearrangements are discussed via the different glass transition shifts observed after atmospheric or high pressure annealing. © 2013 Wiley Periodicals, Inc. J. Appl. Polym. Sci. 000: 000–000, 2013

KEYWORDS: differential scanning calorimetry (DSC); ageing; amorphous; crystallization

Received 31 December 2012; accepted 14 March 2013; Published online 00 Month 2013
DOI: 10.1002/app.39297

INTRODUCTION

Upon cooling, the molecular motion of noncrystallisable amorphous and semi-crystalline polymers sufficiently slows down so that the system departs from the equilibrium state in the melt.[1,2] It gradually solidifies and reaches a metastable glassy state. During annealing at reasonably lower temperature than the glass transition temperature (T_g), the system tends to evolve towards lower energetic states and to get closer to a virtual equilibrium state.[3] This physical-aging process has been widely addressed by volume relaxation experiments[4] or calorimetry. In this latter case, an increase of the glass transition temperature, as well as an endothermic peak located nearby T_g, can be observed after annealing.[5,6] Both the area and location of the peak increase with the annealing time. The densification of the polymer also makes subsequent deformation more difficult.[7–10] Pressure is known to affect the glass transition temperature by freezing earlier the slowest relaxation processes during cooling: T_g increases with pressure by an order of 0.1–0.2 K/MPa in the high-pressure range up to several hundreds of MPa.[6,11,12] The pressure sensitivity was illustrated *in situ* during polymer phase transitions[13,14] *and ex-situ* on solid polymer.[11,15] Furthermore, pressure changes the physical-aging processes and the target state towards which the polymer evolves during annealing, as evidenced by McKinney and Goldstein[16] in PVAc. A major evidence brought by these authors was that the final specific volume reached after pressurizing to a pressure P at $T < T_g$ a glass previously formed at atmospheric pressure P_{atm} is larger than that obtained by forming the glass during cooling down to the same glassy temperature T under P. In the same way, after depressurizing down to P_{atm} a glass previously formed under pressure, the specific volume is smaller than that of the glass directly formed at atmospheric pressure. It means that the volume gain under pressure in the rubbery state keeps relaxed upon cooling down to the glassy state. Following the pioneering work of Goldstein[3] further extended by Stillinger et al.,[17–19] theoretical aspects of glass forming systems have been recently widely discussed from the Potential Energy Landscape (PEL) concept.[20–22,24] The PEL depicts the local and global minima of the potential energy as a function of the configurational coordinates. These minima are separated by transition states over which it is variably frequent to "jump". Although developed for supercooled liquids and small molecules and not for entangled semicrystalline polymers, this formalism brings interesting data to distinguish the temperature and pressure influence on molecular motion. For instance, Middleton and Wales[23] showed that: pressure affects the height of some of the transition states whereas temperature governs the way local energy minima are sampled at fixed energy landscape and the "jump" frequency over transition states.

© 2013 Wiley Periodicals, Inc.

Macromolecules of the semi-crystalline polymer are all in an equilibrium state in the melt. But during crystallization, only some portions of these macromolecules are involved in crystal nucleation and growth. The remaining amorphous portions trap in an out-of-equilibrium state because of the time scales (as depicted above for various glasses) and also because of spatial constraints fixed by connections to the crystal. On the one hand, portions rather disconnected from crystals (e.g., the large interspherulitic domains in weakly crystallized polymers) exhibit a molecular mobility closer to pure amorphous systems, associated with a well-defined glass transition T_g. On the other hand, portions strongly connected to the crystals (e.g., the inter-lamellar layers) explore a strongly reduced number of configurations; moreover, entanglements motions are expected to be very difficult. This fraction remains very constrained even far above the glass transition of the most mobile fraction. In pure amorphous polymers, glass transition was shown to be related yet to a dynamic heterogeneity. This effect is expected to be emphasized in the amorphous part of semi-crystalline polymers.

The amorphous phase of crystalline polymers thus basically displays two modes to gain energy, either by crystallizing or by "aging" the frustrated amorphous phase. The out-of-equilibrium confined amorphous phase[24] tends to evolve towards more stable states upon annealing at constant temperature exceeding the main glass transition T_g. Such evolutions were preferentially tracked by differential scanning calorimetry (DSC)[3,26–32,34–39] in various semicrystalline polymers among which poly-vinylidene fluoride (PVDF),[30] ethylene/1-octene copolymers (EO copolymers),[27] bisphenol A polycarbonate (BAPC),[28,31] nylon 6 (PA6),[33] isotactic polystyrene,[34] and poly-ether-ether-ketone (PEEK).[29,32,35–39] Thermal analysis showed the existence of an endothermic peak, approximately located at the annealing temperature. The peak position and area were shown to depend on the annealing temperature and time. These micro-structural modifications impact the mechanical properties of polymers.[7,40]

Depending on the annealing conditions and authors, these average detected evolutions were variably interpreted. Basically, most of the interpretations can be separated into two views: a "secondary crystallization"[28,29,37] or the "physical-aging"-like evolution of a so-called "rigid amorphous phase" (RAP)[41–43] associated with a proper glass transition (T_{gup}). The former is very often discussed in reference to crystallization from the melt and the latter to physical aging in pure amorphous glassy polymers. Both scenarios are consistent with the calorimetric fingerprint. The discrimination between these two views often lacks quantitative information. For instance, the former scheme implicitly refers to the size and lattice parameters of the nucleated secondary crystals which were barely quantified. Thus, the line may appear very fine between, on one hand, actual small crystals and on the other hand, small domains evolving towards lower energy states (like an out-of-equilibrium constrained amorphous phase). Previous works distinguished two regimes on each side of the crystallization temperature T_c. A primary crystals thickening process was invoked above the crystallization temperature[29] and supported by X-ray diffraction measurements of lamellae thickening.[36] On the other hand, in the temperature range below the crystallization temperature which was preferentially addressed here, the nature of micro-mechanisms is still under discussion. Only a few results, like those brought by Neidhofer et al. by NMR in a polyvinylidene fluoride (PVDF), showed that molecular motions seated in the amorphous phase and not at the vicinity of primary crystals.[30]

Except a recent work by Castagnet and Thilly in polyamide 11 (PA11),[15] the pressure sensitivity of these rearrangements has not been addressed so far. The major contribution of this work is then to focus on annealing pressure, as a parameter affecting the molecular mobility and subsequently the confined amorphous phase rearrangements. This work is carried out in poly-ether-ether-ketone (PEEK). Evolutions are tracked from *ex situ* calorimetry, first after annealing at atmospheric pressure, considering the influence of annealing time and temperature. Then, a similar study is conducted under high-pressure. Finally, attention is paid on the stability of the formed rearrangements by applying two successive annealings for which the annealing temperature or pressure—and thus the molecular mobility—changes. Each set of results is qualitatively discussed through the two above depicted views (secondary crystallization and rigid amorphous phase). Other scenarios would be probably possible but they would need complementary physical characterization.

EXPERIMENTAL

Material

Poly-ether-ether-ketone (PEEK) was received as a $500 \times 500 mm^2$ plate with a thickness of 6 mm, from Goodfellow (Ketron PEEK 1000). The glass transition temperature, the crystallization temperature and the melting temperature of this material are 150, 305, and 340°C, respectively. The degree of cristallinity of the as-received PEEK is about 30%, as estimated from WAXS analysis (Brucker-AXS D8 Advance) in the 2θ range of 11–35°.[36,44]

To avoid skin effects—although they are not very significant (0.5°C on the melting temperature in the 1-mm-thick surface layers)—only the core of the plate is used [Figure 1(a)].

Samples are prepared with two different geometries: samples annealed directly in the DSC apparatus are machined out from a 1-mm-thick band cut from the core of the plate, and samples annealed under hydrostatic pressure in the Paterson press are small cylinders (diameter 14.95 mm; height 6 mm) machined out from the plate. To further characterize these later samples by DSC, they are cut with an Isometh 4000 saw to the DSC sample size [Figure 1(b)].

Differential Scanning Calorimetry

Calorimetry features of microstructure evolutions are characterized in a TA Instruments Differential Scanning Calorimeter Q2000 with Tzero Advanced technology.[45] Tests are operated under dry nitrogen flow (50 mL/min) using a sample mass between 6 and 8 mg. Temperature is calibrated by extrapolating the melting temperature of standards (indium and lead) at 10°C/min. Melting temperature is determined as the endothermic peak maximum temperature recorded at a constant heating

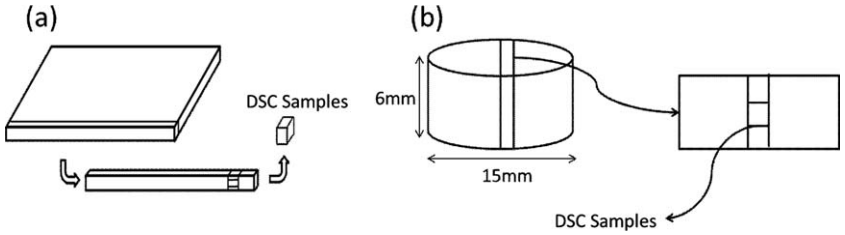

Figure 1. (a) DSC samples preparation from the plate, (b) DSC samples preparation from the Paterson press samples.

rate of 10°C/min. The usual temperature range is from 40 up to 370°C with heating and cooling rates equal to 10°C/min.

The reproducibility was evaluated by investigating three different samples and the variability of the results was negligible, the standard deviation was about of 0.15°C on the peak temperature, each thermogram being obtained with a new specimen. In addition, the baseline of thermograms is subtracted; thermograms are redressed and reduced to zero to be compared more easily to each other. Because of this, the *y*-axis is not represented in the following DSC diagrams.

ANNEALING PROTOCOL

Annealing Under Atmospheric Pressure

Annealings under atmospheric pressure are made *in-situ* in the calorimeter. The annealing protocol is as follows: temperature is raised at 10°C/min from 40°C up to the annealing temperature (T_a) and held at T_a during the annealing time t_a. Then, the sample is cooled down to 40°C at 10°C/min, and the resulting microstructure is characterized: two heating runs are performed between 40°C and 370°C at 10°C/min.

Annealing Under Hydrostatic Pressure

Annealing under hydrostatic pressure is made inside a Paterson press[15] which is an internally heated autoclave ($T < 1400$°C – 50 MPa $< P <$ 500 MPa). No data can be acquired below 50 MPa because of technological constraints with the furnace. To avoid starting the annealing process at atmospheric pressure, pressure is increased up to the annealing pressure (P_a), before temperature is raised up to T_a approximately at 12°C/min. The sample is kept at P_a and T_a during the annealing time t_a. Then, temperature is decreased, prior to pressure. The sample is removed from the Paterson press and the DSC experiment is carried out following the same protocol as described above.

A finite element analysis of heat transfer inside the furnace of the Paterson press was performed in Abaqus, in order to estimate the actual temperature in the sample as a function of the temperature measured at the top with the thermocouple. The full assembly (sample, alumina spacer, alumina piston, zirconia piston and external F_e protection tube) were modeled. A homogeneous heat flux was imposed all around the metal jacket to mimic the temperature evolution recorded during tests. This calculation showed that the difference between temperatures at the thermocouple position and in the middle of samples was about 20°C at the early beginning of heating. It was reduced down to 5°C at the end of the heating ramp. After 2-min equilibrium stage, i.e., at the end of the heating protocol, temperature was uniform in the full assembly.

RESULTS AND DISCUSSION

In order to study the influence of aging during annealing, three characteristics of the DSC diagrams are analyzed: the melting peak, the endothermic peak (through its temperature and area) and the glass transition temperature.

It could be argued that the endothermic peak addressed here arises from a melting-recrystallization-melting process occurring during the DSC scan. It must be underlined that no such peak is observed in the as-received material, whatever on the first or on the second scan. This means that neither the initial material nor that formed during cooling down in the DSC exhibit metastable crystals which would partially melt and recrystallize during the scan. The endothermic peak under consideration only appears after annealing, with characteristics dependent on the annealing conditions, and disappears on the second heating run.

Aging Under Atmospheric Pressure

This section successively considers the influence of the annealing temperature and annealing time at atmospheric pressure. The aim is not so much to characterize finely the phenomenon under atmospheric pressure as to provide a reference for the following investigation of pressure effects.

Influence on Endothermic Peak of Annealing Temperature and Annealing Time

The influence of the annealing temperature T_a is addressed by performing 15-min annealings at 250, 290, and 305°C under atmospheric pressure. Figure 2(a) shows the corresponding DSC thermograms. The evolution of annealing peak temperature and peak area is plotted in Figure 2(b) as a function of the annealing temperature. The enthalpic peak temperature T_{peak} is higher than the annealing temperature T_a. Nevertheless, the gap $\Delta(T_{peak} - T_a)$ decreases from 12°C after annealing at 250°C down to 5°C after annealing at 305°C. The peak area increases from 2.8 to 4.3J/g over the temperature range. Such evolutions suggest that the amorphous phase tends to evolve towards a lower energy state during annealing. This evolution is more and more pronounced when the annealing temperature increases.

The influence of annealing time is studied at atmospheric pressure for a given temperature $T_a = 290$°C; annealing time t_a were 5, 15, 40, 60, and 120 min. Solid lines in Figure 3 show the thermograms associated with these experiments [Figure 3(a)] and the evolution of the annealing peak temperature and area

Applied Polymer SCIENCE

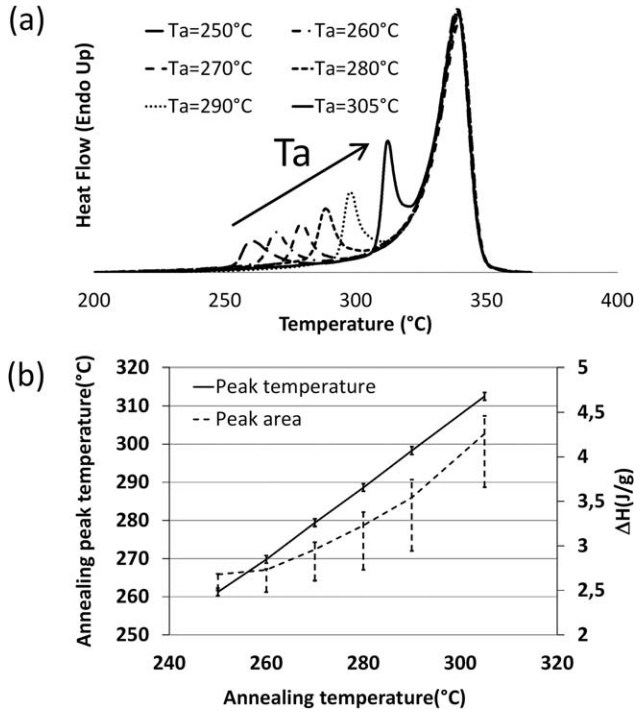

Figure 2. (a) DSC Heating traces after 15 min annealing at various annealing temperatures T_a (250, 260, 270, 280, 290, and 305°C) and (b) dependence of the annealing peak temperature and area on T_a.

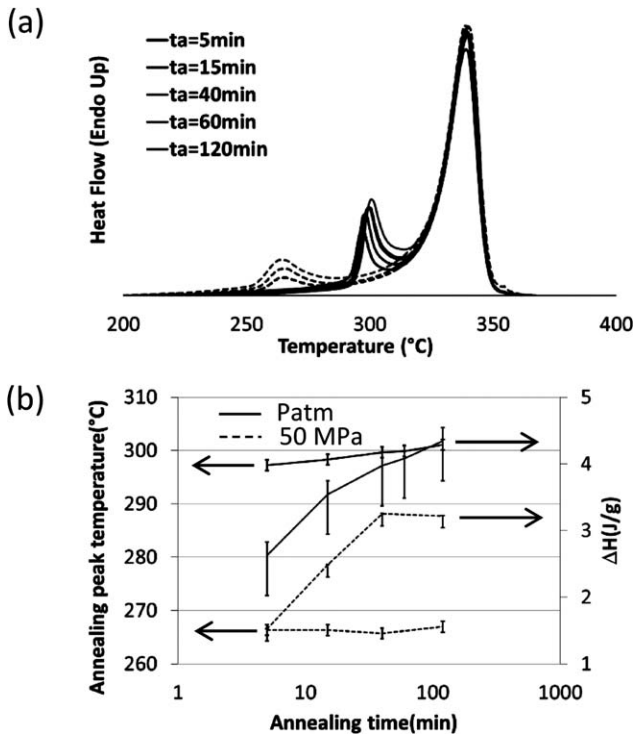

Figure 3. (a) DSC Heating traces after various annealing time (5, 15, 40, 60, and 120 min) at 290°C under P_{atm} (solid) and 50 MPa (short dash) (b) dependence of the annealing peak temperature and area on the annealing time.

as a function of the annealing time [Figure 3(b)]. These results highlight that the aging peak temperature and area both increase with the annealing time. The peak area rises from 2.6 to 4.5 J/g while the annealing peak temperature increases from 297°C to 301°C. Annealing time and temperature have a similar effect on the annealing peak temperature and area, meaning that both parameters influence the amorphous phase evolution towards more stable states. Over the considered ranges, the annealing temperature effect appears more marked than that of the annealing time.

In Figures 2 and 5, no significant variation of the principal melting peak is observed; neither the position of the peak nor the area varies significantly. It evidences that the primary crystalline phase is not affected by the microstructure changes associated with the new endothermic peak.

Consequence on the Most Mobile Fraction of the Amorphous Phase

These first results show an out-of-equilibrium evolution of at least one part of the amorphous phase, but they do not give any information about the "free" amorphous phase evolution which is considered now through the variation of the glass transition temperature (T_g). Figure 4 represents the evolution of T_g versus the annealing time at $T_a = 290$°C, and versus the annealing temperature after 15-min annealing. It shows that the glass transition temperature decreases when annealing temperature increases. Variations of T_g are very close to the experimental scatter and it is difficult to clearly state the annealing time effect. However, a decrease of T_g with the annealing time has already been reported[29,41] and associated with a relaxation of constraints on the amorphous phase.

Discussion About Mechanisms

DSC peaks suggest a global energy gain during annealing, which can be compared to that obtained after physical aging in glassy amorphous polymers, but also to that observed during a crystallization process.

From a "secondary crystallization" view, the increase of the endothermic peak area and temperature could be related to an

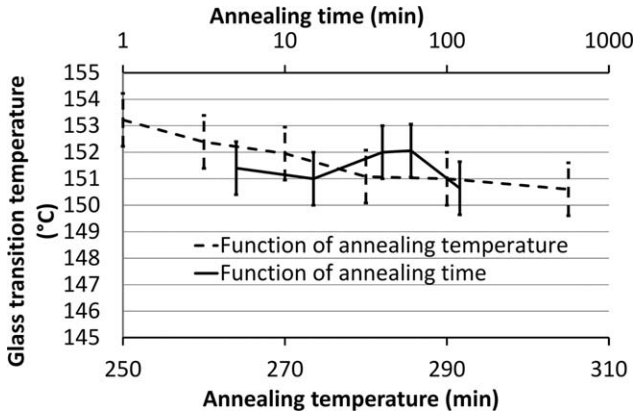

Figure 4. Dependence of the main glass transition temperature on the annealing time at 290°C (top abscissa axis) and on annealing temperature for 15-min annealing (bottom abscissa axis).

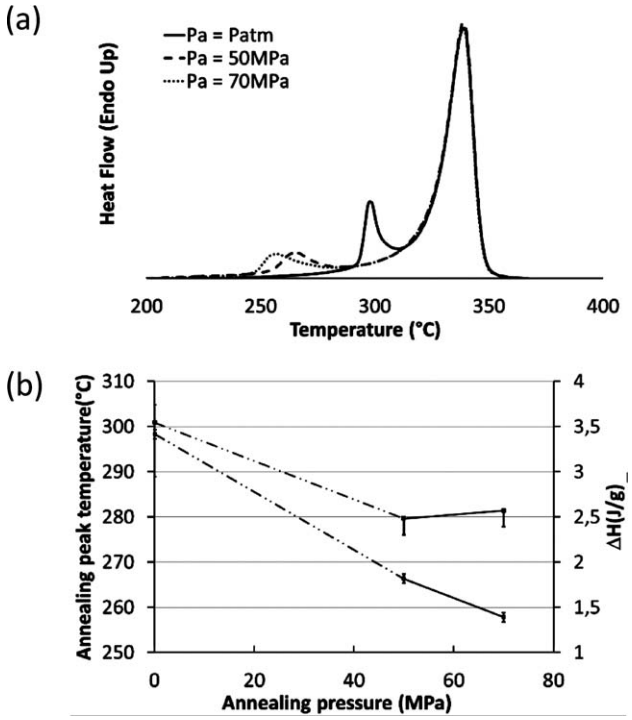

Figure 5. (a) DSC Heating traces after 15 min annealings at 290°C under various annealing pressure (P_{atm}, 50 and 70 MPa) and (b) dependence of the annealing peak temperature and area on the annealing pressure.

increase of the number and size of secondary crystals. It must be reminded that no modification of the primary crystals was noticed. However, the peak area is about 3-4% of the main melting peak area, i.e., about 1% of crystalline fraction. It does not convincingly match with the idea of well-defined crystals all over the amorphous phase. Moreover, despite clear difference about the hypothesis framework, an application of the Gibbs-Thomson relationship between the peak temperature and the crystal thickness leads to only a few crystal units. If so small crystals are nucleated, the distinction between actual "crystals" and rearranged amorphous domains would actually be very tenuous.

From a "rigid amorphous phase" point of view, the increase of the endothermic peak area and temperature could be related to an increase of the number of molecular jumps towards lower energy configurations and to an ability to sample lower energy states in the PEL. The related spatial domains involved in reorganizations would increase with annealing temperature and time. Nevertheless, the area of the annealing peak may appear unusually large compared to that measured after physical-aging in pure amorphous glassy polymers. However, due to the topological constraints related to aromatic cycles in this polymer and considering the coupled pi-stacking process of these cycles,[46,47] it can be reasonably imagined that the amorphous phase can increase local order without actually crystallizing, following the concept of mesophase of Androsch et al.[47] This could explain the large energy gain associated with a marked calorimetric fingerprint. The pi-stacking process is expected to be active during "standard aging" below T_g, but the amount of « stacks » might be much lower due to the highly reduced molecular mobility around compared to the present annealing conditions. Modulated-DSC experiments should be carried out after "standard aging" to quantitatively compare the peak area (convoluted to the C_p jump) to that measured in the present conditions.

Finally, both a secondary crystallization and the physical-aging of a rigid amorphous phase would enhance a relaxation of the most mobile fraction of the amorphous phase. In the latter case, it can be conceived that the amorphous phase could be initially constrained by the pi-stacking process but could be able to relax with time.

Microstructural Evolution Under High Pressure

In this part, aging is performed at 290°C under high pressure in order to quantify the pressure influence on the annealing peak with regard to its position and its area.

Influence of the Annealing Pressure on the Endothermic Peak

To investigate the influence of the annealing pressure, tests are performed between 50 and 70 MPa during 15 min at 290°C. The obtained thermograms, as well as the evolution of the annealing peak temperature and area versus the annealing pressure, are plotted in Figure 5. First, is it clear that the enthalpic peak temperature is much lower than the annealing temperature, the gap $\Delta(T_{peak} - T_a)$ being of −23°C under 50 MPa and −32°C under 70 MPa. The endothermic peak temperature decreases from 297°C at atmospheric pressure down to 258°C under 70 MPa; from this, one can estimate that the high pressure sensitivity is about$\Delta T_{peak}/\Delta P_a = -0.43^{\circ}$C/MPa. Second, the peak area strongly diminishes from 3.5 to 2.5 J/g between atmospheric pressure and 50 MPa, respectively. However, there are no significant differences in peak area between annealing under 50 or 70 MPa. More tests should be performed under 50 MPa to identify the analytical pressure dependence law but this pressure range could not be accessed from our experimental facility, due to technological constraints on the furnace.

High confining pressure thus minimizes local rearrangements in PEEK, as previously evidenced in polyamide 11 (PA11).[15] Microstructure reorganizations do not affect the principal melting peak.

Influence of Annealing Time on the Endothermic Peak

The influence of annealing time under high pressure is considered from a series of annealing experiments at $T_a = 290$°C, $P_a =$ 50 MPa and $t_a = 5$, 15 and 40 min. DSC thermograms are reported in dash lines in Figure 3. Unlike after annealing at atmospheric pressure, the position of the endothermic peak does not change with the annealing time. On the other hand, the peak area increases with the annealing time from 1.5 to 3.3 J/g in a similar way as pointed out at atmospheric pressure.

Effect on Glass Transition Temperature

Unlike after annealing at atmospheric pressure, a significant shift of the glass transition temperature T_g towards higher values is observed after annealing under high pressure in the "rubbery" state. The glass transition temperature increases from 153°C after annealing at atmospheric pressure to 166°C after annealing at 70 MPa. This annealing pressure influence on T_g is

consistent with the annealing temperature influence reported above: an increase of the annealing temperature has the same qualitative influence as a decrease of the annealing pressure. McKinney and Goldstein[16] showed a similar effect of pressure in a pure amorphous polymer, i.e., an increase of the glass transition temperature. The dependence is clearly nonlinear here since T_g increases by 12°C between P_{atm} and 50 MPa and by 1°C only between 50 and 70 MPa.

Relative Importance of Volume and Energy Effects on the Phenomenon

Performing experiments by varying both the annealing temperature and pressure is interesting in that it may help to separate volume effects from purely energy ones. Indeed, a temperature raise both increases the sample volume (and thus reduces molecule interactions so that energy barriers are lowered) and the amount of supplied energy (e.g., larger temperature will enhance dilatation and bring more energy for jumps over barriers). Both effects promote mobility. On the other hand, pressure only affects volume, e.g., decreasing the pressure increases volume and thus barriers, similarly to increasing temperature. But the amount of thermal energy is the same.

Two couples of annealing temperature and annealing pressure, leading to a same volume variation, are extracted from this data. Their total volume variation is estimated from the thermal dilatation from the room temperature (analytically calculated using a first thermal expansion coefficient of $55.10^{-6}K^{-1}$ for temperatures between 23°C and 150°C and a second one of $130.10^{-6}K^{-1}$ for temperatures above 150°C) and a volume change due to mechanical compression (estimated from a compressibility modulus of 5500 MPa). Parameters values are provided by the manufacturer. From this calculation, annealings at (220°C; P_{atm}) and (290°C; 50 MPa) lead to the same volume expansion of 1.61%. A much higher calorimetric signature (temperature and area of the endothermic peak) is observed in the latter case: $T_{peak} = 267$°C and $\Delta H = 2.5$ J/g for the former annealing under 50 MPa at 290°C, against $T_{peak} = 232$°C and $\Delta H = 0.30$ J/g for the annealing at atmospheric pressure and 220°C. This result suggests a stronger energy effect on the reorganization process, but more data should be considered to support this first conclusion.

Discussion About Mechanisms

From the experiments, annealing pressure P_a and temperature T_a can appear as equivalent in that either an increase of T_a or a decrease of P_a lead to a weaker calorimetric signature. However, there are some significant differences between T_a and P_a since temperature both changes the volume and the energy of the system while pressure only changes the volume. The present analysis suggests that the energy effect was predominant over the volume one. Some significant differences between T_a and P_a are also pointed out about the time-evolution of the endothermic peak. Unlike under atmospheric pressure, only the area of the peak was significantly affected by increasing the annealing time. Such a phenomenology suggests that rearrangements under pressure could occur within spatially confined domains and increasing time would lead to better organized microstructures within the same domains.

Can the comparison between annealings under atmospheric and high pressure help to discriminate between physical aging-like processes and crystallization ones? On the first hand, pressure is known to promote nucleation and to increase the crystallization temperature in primary crystallization (i.e., from the liquid to the solid state). When hydrostatic pressure increases, the equilibrium melting temperature is also shifted toward higher temperature values. The crystalline morphology and the number of nuclei are mainly governed by the crystallization supercooling.[48–50] Following this scheme, DSC thermograms after annealings under pressure could be interpreted in terms of nucleation of small crystals which growth would be inhibited because of a weak molecular mobility. The number of nuclei would increase with time but the average size would be unchanged. For increasing pressures at a given annealing temperature, the distance to the effective crystallization temperature would increase and the secondary crystallization process would be less and less detectable. Such a process would constraint the uncrystallized amorphous phase, since T_g increased after annealing under pressure.

On the other hand, pressure is known to raise potential energy barriers in glassy polymers[16,23] and the observed thermograms could be related also to a physical aging-like phenomenon in the constrained amorphous phase. Considering the influence of pressure on the height of energy barriers in PEL studies, it means that the potential energy states sampled at a given thermal energy would be confined within narrower basins under pressure. Reorganized domains could result spatially limited and the endothermic peak located at lower temperature.

Pressure is expected to promote the coupled rearrangement of aromatic cycles: this could explain the significant peak area at short annealing times. Like at atmospheric pressure, the surrounding amorphous phase is expected to be constrained by the pi-stacking process; this would enhance a significant peak for short annealing times. But under pressure, the molecular mobility and the physical-aging ability are reduced (T_g is raised by about 0.1°C/MPa in pure amorphous polymers[6]) and the additional energy gain for longer times is low. Since the constrained and free amorphous phases are interrelated, it could also contribute to the increase of T_g measured after annealing under pressure. It must be underlined that, under pressure, local rearrangements of the amorphous phase occur after partial compaction of the free volume. The microstructure evolves towards a more stable configuration in compacted conditions. Following McKinney and Goldstein's work,[16] the free amorphous phase would return to a smaller equilibrium volume after annealing under pressure and pressure release, than after annealing at atmospheric pressure. Then, the glass transition of this "compacted" phase would be raised. Volume relaxation measurements before and after annealing, as well as physical aging kinetics measurements after annealing, could help to support such an interpretation.

Coexisting Reorganization States

Previous results suggest that annealing promotes a certain degree of "local reorganization" in the material. In this part, the stability of this "local reorganization" is studied by applying successively two annealings, performed under two different

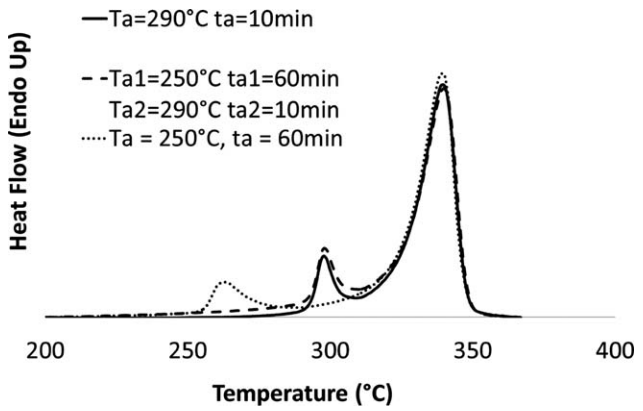

Figure 6. DSC heating traces after two successive annealings at 250°C during 60 min and 290°C during 10 min.

temperature or pressure conditions. The aim is to understand how far each annealing can induce a specific "local reorganization," how far it could be influenced by the previous annealing conditions and how far different reorganization states can interact.

Influence of Variable Annealing Temperature

To investigate the possible coexistence of rearrangements during successive annealings at different temperatures, three tests are performed at atmospheric pressure: (i) a first annealing followed by a second one at higher temperature, (ii) two successive annealings at the same temperature after returning down to the ambient temperature in between, (iii) a first annealing followed by a second one at lower temperature.

i. $T_{a1} < T_{a2}$
In this test, a first annealing at 250°C during 60 min is followed by a second one at 290°C for 10 min. The corresponding thermogram is plotted in Figure 6 and compared with those obtained after single annealing for 10 min at 290°C and for 60 min at 250°C. The first annealing at 250°C would lead to an endothermic peak with a maximum temperature located at 264°C. Such a peak is no longer detected in the double-annealing thermogram. Only one peak at 298°C is observed. It is related to the second annealing signature and almost overlapped with the 290°C single annealing graph. Figure 6 shows that the initial "local organization" promoted at 250°C is erased by increasing temperature during the second annealing. This result can be compared with the removal of the annealing peak during second heating run in the DSC experiment. These results convincingly support the fact that, during a second heating, the lowest energy state is removed.

ii. $T_{a1} = T_{a2}$
The application of two identical annealing temperatures allows a better view of the stability of phases that could be created. Two successive annealings are performed at 290°C after cooling down to the ambient temperature in between. Thermograms perfectly overlap with that of a single annealing. In the case of $t_{a1} = 60$ min and $t_{a2} = 15$ min, $T_{peak} = 300$°C and $\Delta H = 4.17$ J/g; for inversed annealing times $T_{peak} = 300$°C and $\Delta H = 4.19$ J/g; to finish for a single annealing during 75 min at 290°C $T_{peak} = 300$°C and $\Delta H = 4.19$ J/g. Results show that two successive annealings at the same temperature are equivalent to a single one performed during the cumulated time. The local reorganization formed during the first annealing continues during the second one at the same temperature.

iii. $T_{a1} > T_{a2}$
The last tests correspond to a first annealing temperature T_{a1} followed by a second one at lower temperature T_{a2}. The aim is to highlight how the initial "local organization" can interfere with further evolution under more severe conditions regarding molecular mobility. In a first series, the first annealing temperature is varied whereas the first annealing time is changed in the second series. Figure 7(a) displays thermograms of samples submitted to a first 10min annealing at 290, 305, 315, or 325°C, followed by a second one at 250°C during 60 min. The corresponding temperature maximum and area are plotted against the first annealing temperature in Figure 7(b). Two endothermic peaks can be distinguished in each case, meaning that the second annealing does not erase the local reorganization enhanced during the first annealing. Moreover, changes in the first aging peak are similar to those obtained after single annealing at T_{a1}. For a single annealing, $\Delta T_{peak}/\Delta T_a = 0.93$ and in the case of a double annealing $\Delta T_{peak1}/\Delta T_{a1} = 1.00$. Figure 7 shows almost no influence of T_{a1} on the second peak at about 260°C. The temperature associated with the

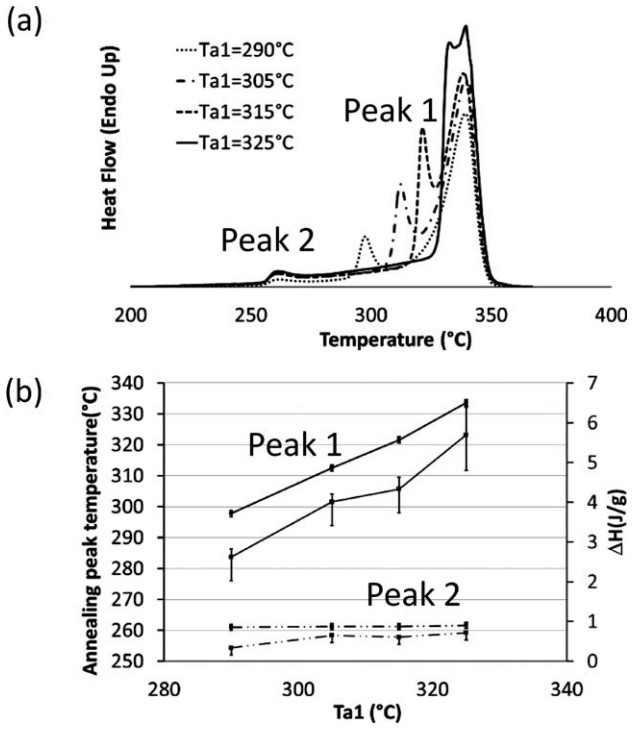

Figure 7. (a) DSC Heating traces after two successive annealings: a first one at 290, 305, 315, or 325°C during 10 min followed by a second one at 250°C during 60 min; (b) dependence of the annealing peak temperature and area for the first (solid) and second (short dash) annealing peak as a function of the first annealing temperature.

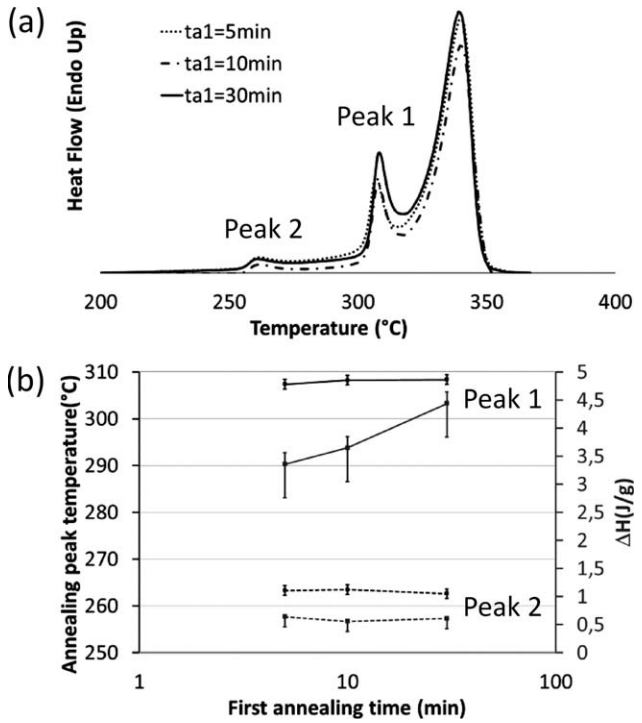

Figure 8. (a) DSC Heating traces after two successive annealings: a first one at 300°C during 5, 10, or 30min followed by a second one at 250°C during 60 min (b); dependence of the annealing peak temperature and area for the first (solid) and second (short dash) annealing peak as a function of the first annealing time.

second peak is not affected and the area only slightly varied, increasing from 0.5 J/g for a first annealing at 290°C to 1 J/g for a first annealing at 325°C. The conclusion is that domains reorganized at T_{a1} remain stable during further annealing at lower temperature and that another form of reorganization takes place at T_{a2}, the latter being rather decoupled from the former one.

Figure 8(a) displays thermograms of samples submitted to a first annealing at 300°C for 5, 10, and 30 min, followed by a second one at 250°C during 60 min like in the first series. The maximum temperature and area of the observed peaks are plotted in Figure 8(b).

Again, two distinct peaks can be observed in each case. The first peak features are similar to those obtained after single annealing in the same conditions, $\Delta T_{peak}/\Delta t_a = 0.07^{\circ}C/min$, $\Delta T_{peak1}/\Delta t_{a1} = 0.04^{\circ}C/min$. Processes activated during the second annealing do not modify the calorimetry characteristics of the first annealing.

Within the investigated domain, the variably achieved reorganization promoted during the first annealing have no consequence on the second reorganization fingerprint at lower temperature. Indeed, the position and the peak area are unaffected. In the case of T_{a1} variations, T_{peak2} value is 262°C and ΔH_2 is around 0.65 J/g. For different t_{a1}, T_{peak2} is 263°C and ΔH_2 is 0.61 J/g.

Again, two co-existing but noninteracting processes are activated during the two successive annealings.

Influence of the Annealing Pressure

Pressure effects are also analyzed in case of double annealing. In the same way as previously addressed with temperature, two double-annealing tests at successive pressures are performed. The goal is again to evaluate how far a first reorganization process can be affected by a second one, performed under less severe conditions regarding molecular mobility. To this aim, the second annealing pressure is lower than the first one.

The first annealing temperature T_{a1}, time t_{a1}, and pressure P_{a1} are set at 290°C, 15 min and 70 MPa for both tests, respectively. The second annealing occurs at $T_{a2} = 290^{\circ}C$ and $t_{a2} = 15$ min for both tests. The second annealing pressure P_{a2} is either 50 MPa or the atmospheric pressure.

Thermograms of these experiments (double annealings and reference single annealing under 70 MPa) are presented in Figure 9. When performing a second annealing at atmospheric pressure the "ordering" performed under 70 MPa is erased. This observation is consistent with the results on double annealing with $T_{a1} < T_{a2}$ if considering that temperature and pressure qualitatively affect the molecular mobility in equivalent ways. Indeed, an increase of the annealing temperature lead to similar calorimetry features as a decrease of the annealing pressure. However, when the second annealing is performed under 50 MPa, there is neither elimination nor even significant modification of the first annealing peak. The peak temperature is almost the same for a single annealing at 70 MPa or a double annealing with $P_{a1} = 70$ MPa and $P_{a2} = 50$ MPa. This result could mean that the diminution of the pressure (70–50 MPa) is not enough to observe a real influence on the "local reorganization".

Discussion About Mechanisms

After a second annealing in less favorable conditions for molecular mobility (i.e., by raising pressure or decreasing temperature), an additional endothermic peak is observed at lower temperature. From a "crystallization" view, it could mean that a second population of small crystals, may be smaller and less stable than the first one, would be nucleated. In a "physical-aging"

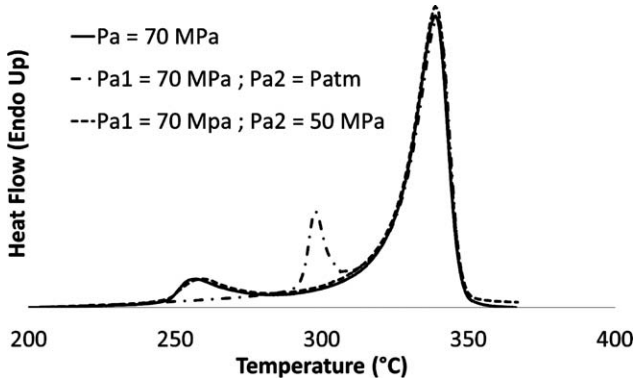

Figure 9. DSC Heating traces for double annealing, first annealing at 290°C during 15 min under 70 MPa, and second one at 290°C under 50 MPa and P_{atm} during 15 min, and for one annealing at 70 MPa.

process of the rigid amorphous phase, it could mean that the pi-stacking process already occurred during the first annealing and that the additional energy gain is much smaller during second annealing, and closer to the usual order of energy involved in physical aging of pure glassy amorphous polymers.

Second annealing at increased molecular mobility (i.e., by raising temperature or decreasing pressure), confirms that an energy-lowered microstructure is destroyed by the thermal energy supplied during further heating above the annealing temperature. It can be evidenced for instance by the vanishing of the endothermic peak observed during second heating run in DSC tests. From a "physical-aging"-like view, molecular jumps could be activated above higher energy barriers and reorganized domains would be no longer stable. During the first annealing, potential energy minima with a given energy depth would be sampled, allowing finite local rearrangements. Upon heating, thermal vibration increase so that the previous energy barrier could now be overcome and that there would be no more detectable energy difference between rearranged domains and others. When decreasing the annealing pressure, such jumps could be possible because of the decrease of energy barriers. Nevertheless, since energy effects are more pronounced than volume ones, a huge pressure decrease is needed to make the process visible. For instance, a 20 MPa depression between successive annealings is not sufficient to erase the first reorganized state. In a "secondary crystallization" view, it can be easily conceived that an increase of temperature make the crystal melt. Crystals formed at a given pressure and temperature would become unstable when re-heated up to the same temperature but lower pressure, provided that the pressure gap is large enough. For instance, a pressure difference of 20 MPa here is not sufficient for annealings at 290°C.

After cumulated annealings at the same temperature T_a, the resulting endothermic peak overlap with that obtained after one single annealing performed during the cumulated time. From a "physical-aging"-like view, the energy minimization process would depend on the injected thermal energy, with a kinetics related to the amount of molecular jumps cumulated with time. From a "secondary crystallization" view, this result means that entities nucleated during the first annealing do not promote nucleation during the second one (i.e., do not act as pre-existing nuclei) and do not accelerate the kinetics during the second annealing. It seems questionable for a nucleation/growth process.

CONCLUSIONS

This study addressed the out-of-equilibrium evolutions of PEEK microstructure during annealing above the main glass transition temperature. The two major objectives were to investigate (i) the pressure sensitivity of observed phenomena and (ii) the stability of co-existing rearrangements during successive annealings at different temperatures or pressures. Results at atmospheric pressure were consistent with those previously reported in several semi-crystalline polymers. An endothermic peak appeared in DSC scans, above the annealing temperature. Both the maximum temperature and the area of this peak increased with the annealing time. The expectedly large area of the peak, compared to physical aging in pure glassy polymers, could arise from a pi-stacking process of aromatic cycles.

Annealing temperature and pressure could be regarded as equivalent parameters, mostly because a decrease in the annealing temperature or an increase in the annealing pressure reduced or even prevented any calorimetric signature of microstructure rearrangements. However, temperature and pressure did not have the same impact on rearrangement processes. The location and area of DSC peaks suggested that rearrangements activated under pressure affected confined domains, more and more stable with time, while those occurring at atmospheric pressure could extend to larger domains with time.

Rearrangements enhanced during a first annealing were erased by subsequently submitting the material to conditions promoting molecular mobility, i.e., by increasing temperature or decreasing pressure. In the opposite way, more restricted but distinct rearrangements arose from applying more severe subsequent annealing conditions, for instance by decreasing the annealing temperature.

Microstructure rearrangements towards a less energetic state did not affect the melting temperature of primary crystals, but modified the free amorphous phase which appeared to be relaxed during annealing at atmospheric pressure and stabilized in a denser state during annealing under pressure. More generally, extension of the annealing conditions to variable pressure showed that microstructure rearrangements in the most mobile and the most constrained fractions of the amorphous phases were related to each other. It supported the idea that a drastic separation between two independent "free and rigid" amorphous phases—like often assumed in multiscale inclusion modeling for semi-crystalline polymers—was not accurate for long-term loadings.

Authors gratefully acknowledge fruitful discussions with Dr. J.L. Gacougnolle. The French Ministry of Research is also acknowledged for granting M. Dasriaux's PhD.

REFERENCES

1. McKenna, G. B. *Comp. Mater. Sci.* **1995**, *4*, 349.
2. Mileva, D.; Zia, Q.; Androsch, R.; Radusch, H.; Piccarolo, S. *Polymer* **2009**, *50*, 5482.
3. Goldstein, M. *J. Chem. Phys.* **1969**, *51*, 3728.
4. Kovacs, A. *J. Polym. Sci.* **1958**, *30*, 131.
5. Kemmish, D. J.; Hay, J. N. *Polymer* **1985**, *26*, 905.
6. Bianchi, U. *J. Phys. Chem.* **1965**, *69*, 1497.
7. Struik, L. C. E. Physical Aging in Amorphous Polymers and Other Materials, Elsevier Science, **1980**; p 244.
8. Plazek, D. *J. Phys. Chem.* **1965**, *69*, 3480.
9. Bernatz, K. M.; Giri, L.; Simon, S. L.; Plazek, D. J. *J. Chem. Phys.* **1999**, *111*, 2235.

10. Cheriere, J.; Belec, L.; Gacougnolle, J. *Polym. Eng. Sci.* **1997**, *37*, 1664.
11. Paterson, M. S. *J. Appl. Phys.* **1964**, *35*, 176.
12. Schwartz, G. A.; Paluch, M.; Alegría, A; Colmenero, J. *J. Chem. Phys.* **2009**, *131*, 044906.
13. Hohne, G. W. H.; Rastogi, S.; Wunderlich, B. *Polymer* **2000**, *41*, 8869.
14. Boyer, S. A. E.; Grolier, J. P. E.; Yoshida, H.; Iyoda, T. *J. Polym. Sci. Part B-Polym. Phys.* **2007**, *45*, 1354.
15. Castagnet, S.; Thilly, L. *J. Polym. Sci. Part B-Polym. Phys.* **2009**, *47*, 2015.
16. McKinney, J. E.; Goldstein, M. *J. Res. Natl. Bureau Std. Section A-Phys. Chem.* **1974**, *78*, 331.
17. Stillinger, F. H. *Science* **1995**, *267*, 1935.
18. Debenedetti, P. G.; Stillinger, F. H. *Nature* **2001**, *410*, 259.
19. Debenedetti, P. G.; Stillinger, F. H.; Truskett, T. M.; Lewis, C. P. *Adv. Chem. Eng.* **2001**, *28*, 21.
20. Chung, Y. G.; Lacks, D. J. *Macromolecules* **2012**, *45*, 4416.
21. Mossa, S.; Sciortino, F. *Phys. Rev. Lett.* **2004**, *92*, 4.
22. Rehwald, C.; Gnan, N.; Heuer, A.; Schroder, T.; Dyre, J. C.; Diezemann, G. *Phys. Rev. E* **2010**, *82*, 1.
23. Middleton, T. F.; Wales, D. J. *J. Chem. Phys.* **2003**, *118*, 4583.
24. Heuer, A. *J. Phys.-Condens. Matter* **2008**, *20*, 37.
25. Flory, P. J. *J. Am. Chem. Soc.* **1962**, *84*, 2857.
26. Loufakis, K.; Wunderlich, B. *Macromolecules* **1987**, *20*, 2474.
27. Alizadeh, A.; Richardson, L.; Xu, J.; McCartney, S.; Marand, H.; Cheung, Y.; Chum, S. *Macromolecules* **1999**, *32*, 6221.
28. Alizadeh, A.; Sohn, S.; Quinn, J.; Marand, H.; Shank, L.; Iler, H. *Macromolecules* **2001**, *34*, 4066.
29. Marand, H.; Alizadeh, A.; Farmer, R.; Desai, R.; Velikov, V. *Macromolecules* **2000**, *33*, 3392.
30. Neidhofer, M.; Beaume, F.; Ibos, L.; Bernes, A.; Lacabanne, C. *Polymer* **2004**, *45*, 1679.
31. Sohn, S.; Alizadeh, A.; Marand, H. *Polymer* **2000**, *41*, 8879.
32. Velikov, V.; Marand, H. *J. Thermal Anal.* **1997**, *49*, 375.
33. Chen, H.; Cebe, P. *J. Thermal Anal. Calorimetry* **2007**, *89*, 417.
34. Xu, H.; Cebe, P. *Macromolecules* **2004**, *37*, 2797.
35. Wei, C. L.; Chen, M.; Yu, F. E. *Polymer* **2003**, *44*, 8185.
36. Blundell, D. J. *Polymer* **1987**, *28*, 2248.
37. Fougnies, C.; Damman, P.; Dosiere, M.; Koch, M. H. J. *Macromolecules* **1997**, *30*, 1392.
38. Fougnies, C.; Damman, P.; Villers, D.; Dosiere, M.; Koch, M. H. J. *Macromolecules* **1997**, *30*, 1385.
39. Buggy, M.; Carew, A. *J. Mater. Sci.* **1994**, *29*, 2255.
40. Brennan, A. B.; Feller, F. *J. Rheol.* **1995**, *39*, 453.
41. Huo, P. T.; Cebe, P. *Macromolecules* **1992**, *25*, 902.
42. Lu, S. X.; Cebe, P. *Polymer* **1996**, *37*, 4857.
43. Wunderlich, B. *Prog. Polym. Sci.* **2003**, *28*, 383.
44. Hay, J. N.; Kemmish, D. J.; Langford, J. I.; Rae, A. I. M. *Polym. Commun.* **1984**, *25*, 175.
45. Danley, R. L. *Thermochimica Acta* **2003**, *395* (1-2), 201.
46. Strobl, G. *Eur. Phys. J. E* **2000**, *3*, 165.
47. Androsch, R.; Di Lorenzo, M. L.; Schick, C.; Wunderlich, B. *Polymer* **2010**, *51*, 4639.
48. Won, J. C.; Fulchiron, R.; Douillard, A.; Chabert, B.; Varlet, J.; Chomier, D. *J. Appl. Polym. Sci.* **2001**, *80*, 1021.
49. Bhateja, S. K.; Pae, K. D. *J. Macromol. Sci.-Rev. Macromol. Chem. Phys.* **1975**, *C13*, 77.
50. Boyer, S. A. E.; Haudin, J. M. *Rev. Sci. Instrum.* Submitted.